Cage effect for the velocity correlation functions of a Brownian particle in viscoelastic shear flows

Romi Mankin, Katrin Laas,* Neeme Lumi, and Astrid Rekker
Institute of Mathematics and Natural Sciences, Tallinn University, 29 Narva Road, 10120 Tallinn, Estonia
(Received 3 August 2014; published 20 October 2014)

The long-time limit behavior of velocity correlation functions (VCFs) for an underdamped Brownian particle in an oscillatory viscoelastic shear flow is investigated using the generalized Langevin equation with a power-law memory kernel. The influence of a fluctuating environment is modeled by an additive external fractional Gaussian noise. The exact expressions of the correlation functions of the fluctuating components of velocity for the Brownian particle in the shear plane have been calculated. Also, the particle's angular momentum is found. It is shown that in a certain region of the system parameters an interplay of the shear flow, memory effects, and external noise can induce a bounded long-time behavior of the VCFs, even in the shear flow direction, where in the case of internal noise the velocity process is subdiffusive, i.e., unbounded in time. Moreover, we find resonant behavior of the VCFs and the angular momentum versus the shear oscillation frequency, implying that they can be efficiently excited by oscillatory shear. The role of the initial positional distribution of particles is also discussed.

DOI: 10.1103/PhysRevE.90.042127 PACS number(s): 05.40.−a, 02.50.−r, 83.50.Ax

I. INTRODUCTION

Diffusion of mesoscopic particles suspended in simple solvents, governed by Brownian motion, is one of the pillars of biological and soft condensed matter physics [1]. Moreover, experiments from many different areas reveal that anomalous diffusion with a mean-square displacement of particles $\langle \boldsymbol{r}^2(t)\rangle \sim t^{\alpha}$, $(\alpha \neq 1)$ is ubiquitous in nature, signaling that slow transport, $(\alpha < 1)$, may be generic for complex heterogeneous materials [1]; examples are colloidal suspensions, glasses, polymer solutions [2,3], viscoelastic media, amorphous semiconductors [4–6], cytoplasm of living cells [7], large proteins [8], and dusty plasmas [9]. It is well known that a stochastic force (noise) can modify the behavior of complex systems in a counterintuitive way and thus induce unexpected ordered outcomes such as ratchet effect [10–12], stochastic resonance [13–15], hypersensitive transport [16–18], etc. Also, the phenomenon of anomalous diffusion can be considered as a noise-generated effect via the framework of the generalized Langevin equation (GLE) [19–23].

Since optically trapped particles are more suited for a thorough statistical analysis of their Brownian dynamics, several works have recently been focused on the dynamics of underdamped Brownian particles trapped by harmonic potentials and exposed to shear flows [24–29]. Particularly, it has been shown that the particle position distribution takes an elliptical shape and shear-induced cross-correlations occur between particle fluctuations along orthogonal directions in the shear plane [25,29]. Moreover, analytical solutions exposed in Ref. [28] for an oscillatory shear flow reveal that the particle distribution and the cross-correlations exhibit a strong resonance in weakly damped systems. However, in Refs. [24–29] it is assumed that the interaction of Brownian particles with shear flow is characterized by Stokes friction. The latter is irrelevant for shear flows in viscoelastic media, where anomalous diffusion occurs [4,30]. To overcome part of the last mentioned problem, the authors of Ref. [31] have considered a GLE with a power-law memory kernel, which models the dynamics of an underdamped Brownian particle in a fluctuating harmonic potential well subjected to an oscillatory viscoelastic shear flow. The influence of a fluctuating environment is modeled by a multiplicative white noise and by an internal fractional Gaussian noise. It is shown that an interplay of shear flow, memory, and multiplicative noise can generate a variety of cooperation effects, such as energetic instability, multiresonance versus the shear frequency, memory-induced anomalous diffusion, etc.

However, Ref. [31] leaves open an important question, from both the theoretical and experimental viewpoints, namely, what happens if internal noise is replaced either with an additive external noise or with a superposition of internal and external noises. It is well known that in the case of internal noise the dynamics of a Brownian particle described with a GLE in quiescent viscoelastic fluids is substantially different from the case of external noise [20,32–34]. Particularly, in the presence of an external noise the phenomenon of memory-induced trapping occurs; i.e., at sufficiently small values of the memory exponent a stationary regime of the particle's dynamics is possible even if the trapping potential well in the GLE is absent [33,34]. If the additive noise is internal, such self-trapping of a free particle is impossible and the particle's dynamics is subdiffusive [20]. A physical explanation for this interesting result is based on the cage effect (see, e.g., Ref. [23]).

Motivated by reasons represented above and by the results of Ref. [31] the present paper considers a model similar to the one presented in Ref. [31], except that the fluctuating harmonic trapping potential in the GLE is absent (i.e., we consider a free particle) and that the internal noise is replaced with an additive external Gaussian fractional noise. Note that in intracellular microrheology experiments it has been observed that the fluctuating force of the collective action of the molecular motors on a diffusing particle exhibits a power spectrum with a power-law behavior [32,35–37]. For example, in Ref. [32] the authors have succeeded in modeling the collective action of the molecular motors as an external fractional noise in a GLE, obtaining results which are in agreement with experimental data.

*katrin.laas@tlu.ee

The main contribution of this paper is as follows. In the long-time limit, $t \to \infty$, we provide exact formulas for the analytic treatment of the dependence of the velocity correlation functions (VCF) on the lag time and on the shear frequency. Here we emphasize that in experiments information about the observed dynamical behavior of particles is usually extracted from the VCFs and/or from the mean-square displacement [1,32,35–39]. We have established two critical exponents characterizing the memory kernel and the external noise, which mark the dynamical transition due to the cage effect from a state with unbounded (in time) VCFs to one with bounded VCFs. This is in contrast to the case of internal noise, where the particle's velocity process in the direction of the shear flow is always subdiffusive (i.e., unbounded in time). Based on exact expressions of VCFs in the bounded regime, we show that in the long lag-time limit, $\tau \to \infty$, the velocity autocorrelation function in the shear flow direction does not vanish but demonstrates an oscillatory behavior with a finite amplitude which depends on the shear flow frequency Ω and on the initial positional distribution of particles. Moreover, we have found that the amplitudes of the asymptotic velocity cross-correlation functions and the velocity autocorrelation function in the shear flow direction exhibit a clear resonance at a value of Ω which depends only on the parameters of the memory kernel. Furthermore, we will show that in certain parameter regions an interplay of the shear flow and memory effects can generate a multiresonance of the second-order moments of the particle velocity components versus Ω and a resonance of the mean angular momentum versus Ω.

The structure of the paper is as follows. In Sec. II we present the model investigated. In Sec. III exact formulas are found for the velocity correlation functions. We analyze the dependence of the VCFs on the system parameters and on the time lag. In Sec. IV the resonant behavior of the second-order moments of the velocity and of the mean angular momentum is considered. Section V contains some brief concluding remarks. Some formulas are delegated to the Appendixes.

II. MODEL AND THE EXACT MOMENTS

A. Model

Following Ref. [31], we consider a Brownian particle of the unit mass ($m = 1$) suspended at the position $\boldsymbol{r} = (X,Y,Z)$ in a viscoelastic flow field with parallel streamlines in the x direction

$$\boldsymbol{v}(\boldsymbol{r},t) = \rho Y \cos(\Omega t)\boldsymbol{e}_x, \tag{1}$$

with $\boldsymbol{e}_x$ denoting the unit vector in the x direction, ρ the shear rate, and Ω the shear frequency. As a model for such a system with memory, strongly coupled with a noisy environment, we consider a GLE,

$$\ddot{\boldsymbol{r}}(t) + \gamma \int_0^t \eta(t-t')\{\dot{\boldsymbol{r}}(t') - \boldsymbol{v}[\boldsymbol{r}(t'),t']\}\,dt' = \boldsymbol{\xi}(t), \tag{2}$$

where $\dot{\boldsymbol{r}} \equiv d\boldsymbol{r}/dt$, γ is a damping coefficient, $\eta(t)$ is the dissipative memory kernel that characterizes the viscoelastic properties of the medium, and $\boldsymbol{\xi}(t) = [\xi_1(t),\xi_2(t),\xi_3(t)]$ is an external random force representing the action of nonthermal fluctuations, i.e., the noise $\boldsymbol{\xi}(t)$ is not related to the memory kernel $\eta(t)$ via the fluctuation-dissipation theorem [40]. In what follows we will assume that the driving noise $\boldsymbol{\xi}(t)$ is a stationary, zero-centered ($\langle\boldsymbol{\xi}\rangle = 0$), fractional Gaussian noise with correlation functions given by

$$C_{ij}(\tau) \equiv \langle \xi_i(t+\tau)\xi_j(t)\rangle = \delta_{ij}\frac{2D}{\Gamma(1-\delta)}\frac{1}{\tau^\delta}, \tag{3}$$

where $0 < \delta < 1$, D characterizes the noise intensity, $\Gamma(1-\delta)$ is the Γ function, and δ_{ij} is the Kronecker symbol. To reproduce the viscoelastic properties of the medium, the dissipative kernel $\eta(t)$ is supposed to be a power-law memory [19–23]:

$$\eta(t) = \frac{1}{\Gamma(1-\alpha)t^\alpha}, \quad 0 < \alpha < 1. \tag{4}$$

By taking the limit $\alpha \to 1$ in Eq. (4) we see that $\eta(t)$ possesses all properties of the δ function (its δ-functional behavior manifests itself in the integrals), and thus $\eta(t)$ at $\alpha \to 1$ corresponds to nonretarded friction (Stokes friction) in the GLE (2). It is worth mentioning that in the case without the flow field $\boldsymbol{v}(\boldsymbol{r},t)$ the counterparts of the model (2) with Eqs. (3) and (4) are widely used in fitting experimental data from intracellular microrheology [21,22,32]. For example, as pointed out in Ref. [32], intracellular transport of large proteins, vesicles, etc., is a complex dynamical process that involves an interplay of adenosine triphosphate (ATP) consuming molecular motors, cytoskeleton filaments, and the viscoelastic cytoplasm. The irreversible conversion of chemical energy from ATP hydrolysis (a stochastic process) into particle motion via the activity of myosin-V motors drives the system out of equilibrium [32]. As a consequence the corresponding noise in the GLE, which models the process, is an external noise. Moreover, in recent experiments it has been observed that the forces power spectrum exhibits a power-law behavior [32,35–37]. This circumstance is one of our motivations to consider the GLE (2) with assumptions (3) and (4).

B. First moments

Due to the linearity of Eq. (2) the z component of $\boldsymbol{r}(t)$ decouples, and the process $Z(t)$ behaves as a one-dimensional fractional oscillator considered in Ref. [34]. Therefore, in the rest of this paper we will consider the motion in the xy plane. In the xy plane the GLE (2) can be written as two second-order fractional differential equations:

$$\ddot{Y}(t) + \gamma \frac{d^\alpha}{dt^\alpha}Y(t) = \xi_2(t), \tag{5}$$

$$\ddot{X}(t) + \gamma \frac{d^\alpha}{dt^\alpha}X(t) = \xi_1(t) + \gamma\rho\,\frac{d^\alpha}{dt^\alpha}\left[\int_0^t Y(t')\cos(\Omega t')\,dt'\right], \tag{6}$$

where the operator d^α/dt^α with $0 < \alpha < 1$ denotes the fractional derivative in Caputo's sense, given by [41]

$$\frac{d^\alpha f(t)}{dt^\alpha} = \frac{1}{\Gamma(1-\alpha)}\int_0^t \frac{\dot{f}(t')}{(t-t')^\alpha}\,dt'. \tag{7}$$

By applying the Laplace transformation to Eqs. (5) and (6) one can easily obtain formal expressions for the displacements

$X(t)$ and $Y(t)$ in the following forms:

$$Y(t) = \langle Y(t)\rangle_\xi + \int_0^t H(t-t')\xi_2(t')\,dt', \tag{8}$$

$$X(t) = \langle X(t)\rangle_\xi + \int_0^t H(t-t')\left\{\xi_1(t') + \gamma\rho\frac{d^\alpha}{dt'^\alpha} \times\left[\int_0^{t'}(Y(\tau)-\langle Y(\tau)\rangle_\xi)\cos(\Omega\tau)\,d\tau\right]\right\}dt', \tag{9}$$

where the averages over an ensemble of realizations of the noise $\boldsymbol{\xi}(t)$, $\langle Y(t)\rangle_\xi$, and $\langle X(t)\rangle_\xi$ are given by

$$\langle Y(t)\rangle_\xi = \dot{y}_0 H(t) + y_0, \tag{10}$$

$$\langle X(t)\rangle_\xi = \dot{x}_0 H(t) + x_0 - \frac{\rho y_0}{\Omega}\int_0^t \ddot{H}(t')\sin[\Omega(t-t')]\,dt' + \rho\dot{y}_0\int_0^t [1-\dot{H}(t-t')]H(t')\cos(\Omega t')\,dt', \tag{11}$$

with the deterministic initial conditions $X(0) = x_0$, $Y(0) = y_0$, $\dot{X}(0) = \dot{x}_0$, and $\dot{Y}(0) = \dot{y}_0$. The relaxation function $H(t)$ can be represented as

$$H(t) = t\,E_{2-\alpha,2}(-\gamma t^{2-\alpha}), \tag{12}$$

where $E_{\eta,\mu}(z)$ is the generalized Mittag-Leffler function [41]:

$$E_{\eta,\mu}(z) = \sum_{n=0}^{\infty}\frac{z^n}{\Gamma(n\eta+\mu)}. \tag{13}$$

For large t the function $H(t)$ decays as a power law, namely, at $t\to\infty$,

$$H(t) \simeq \frac{1}{\gamma\Gamma(\alpha)t^{1-\alpha}}. \tag{14}$$

Thus, in the long-time limit, $t\to\infty$, the mean values of the particle displacement and velocity relax to

$$\langle X\rangle_{\xi as} := \langle X\rangle_{\xi|t\to\infty} = x_0 - \frac{\rho y_0}{\Omega}|\widehat{\ddot{H}}(-i\Omega)|\sin(\Omega t+\varphi) + \rho\dot{y}_0\,\mathrm{Re}[\widehat{H}(-i\Omega)], \tag{15}$$

$$\langle Y\rangle_{\xi as} := \langle Y\rangle_{\xi|t\to\infty} = y_0, \tag{16}$$

$$\langle\dot{X}\rangle_{\xi as} := -\rho y_0|\widehat{\ddot{H}}(-i\Omega)|\cos(\Omega t+\varphi), \quad \langle\dot{Y}\rangle_{\xi as} := 0, \qquad \Omega\neq 0, \tag{17}$$

where the phase shift φ can be represented as

$$\tan\varphi = -\frac{\mathrm{Im}[\widehat{\ddot{H}}(-i\Omega)]}{\mathrm{Re}[\widehat{\ddot{H}}(-i\Omega)]}, \tag{18}$$

and $\widehat{H}(s)$ is the Laplace transform of $H(t)$, i.e.,

$$\widehat{H}(s) = \int_0^\infty e^{-st}H(t)\,dt. \tag{19}$$

From Eqs. (15)–(17) it can be seen that the initial value of the velocity influences only the mean value of the x coordinate of the particle position, but not the y coordinate and the mean velocity. In the following, we assume (from an experimental point of view, a reasonable assumption) that the initial values are statistically independent random quantities with zero mean and finite (constant) variance, i.e.,

$$\langle x_0\rangle = \langle y_0\rangle = \langle\dot{x}_0\rangle = \langle\dot{y}_0\rangle = 0. \tag{20}$$

Obviously, in this case we get

$$\langle X(t)\rangle = \langle Y(t)\rangle = \langle\dot{X}(t)\rangle = \langle\dot{Y}(t)\rangle = 0, \tag{21}$$

where the brackets $\langle\rangle$ denote an average over an ensemble of realizations of the noise $\boldsymbol{\xi}(t)$ and over the initial conditions $(x_0, y_0, \dot{x}_0, \dot{y}_0)$.

To avoid misunderstanding, note that we use the symbols "$\sim$" and "$\simeq$" for denoting asymptotically proportional to and asymptotically equal to, respectively.

III. VELOCITY CORRELATION FUNCTIONS

In the following, our interest is focused on the long-time regime, $t\to\infty$. We consider the following VCFs: $C_{11}^V \equiv \langle\dot{Y}(t)\dot{Y}(t+\tau)\rangle_{as}$, $C_{12}^V \equiv \langle\dot{X}(t)\dot{Y}(t+\tau)\rangle_{as}$, $C_{21}^V \equiv \langle\dot{X}(t+\tau)\dot{Y}(t)\rangle_{as}$, and $C_{22}^V \equiv \langle\dot{X}(t+\tau)\dot{X}(t)\rangle_{as}$ that determine the particle's velocity distribution function (see Refs. [25,28]). Since the motion in the y direction is independent of the shear flow and of the motion in the x direction, the respective correlation functions remain unaffected. These are simply those of a fractional oscillator and can be found as in Refs. [33,34]. In particular, in the long-time regime

$$\langle Y(t+\tau)Y(t)\rangle_{as} = \langle y_0^2\rangle + 2D\psi(\tau), \tag{22}$$

$$\langle\dot{Y}(t+\tau)\dot{Y}(t)\rangle_{as} = -2D\ddot{\psi}(\tau), \tag{23}$$

where

$$2D\psi(\tau) = \int_0^t H(t')M(t'+\tau)\,dt' + \int_0^t H(t'+\tau)M(t')\,dt', \quad t\to\infty, \tag{24}$$

and the involved function M is given by [see Eqs. (3) and (8)]

$$M(t) = \int_0^t H(t-t')C_{22}(t')\,dt'. \tag{25}$$

Another representation of $\psi(\tau)$, more convenient for numerical calculations and for analysis of the asymptotic behavior, is given by Eqs. (A1)–(A6) in Appendix A.

The behavior of other VCFs depends strongly on the character of the function $\psi(\tau)$. Particularly, if the exponents δ and α are such that

$$1 > \delta > 2\alpha, \tag{26}$$

the process $Y(t)$ is, in the long-time limit, $t\to\infty$, stationary and $\psi(\tau)$ depends only on the lag time τ (see also Appendix A). In this case at $\tau\to\infty$, the asymptotic behavior of $\psi(\tau)$ reads

$$\psi(\tau) \simeq \frac{\Gamma(\delta-2\alpha)}{\pi\gamma^2\tau^{\delta-2\alpha}}\{\sin[\pi(\delta-\alpha)] + \sin(\pi\alpha)\}; \tag{27}$$

i.e., it demonstrates a power-law decay. If the condition (26) is not fulfilled, then the process $Y(t)$ is not stationary, demonstrating anomalous diffusion [see Eq. (A4)] and $\psi(\tau)$

depends on both times t and τ, increasing in the long-time limit as

$$\psi(\tau,t) \sim t^{2\alpha-\delta}, \quad t \to \infty, \quad \delta < 2\alpha. \tag{28}$$

Notably, in the case of internal noise, $\alpha = \delta$, the process $Y(t)$ is subdiffusive with $\psi(\tau,t) \sim t^{\alpha}$, $t \to \infty$. In the rest of this paper we assume that the condition (26) is fulfilled, i.e., $Y(t)$ is a stationary process. Now we obtain analytical expressions for the VCFs. From Eqs. (8), (9), and (22) we get

$$\langle \dot{Y}(t+\tau)\dot{X}(t)\rangle_{as} = -2D\rho \mathrm{Re}\left[e^{i\Omega t}\int_0^t e^{-i\Omega t_1}\ddot{H}(t_1)\dot{\psi}(t_1+\tau)\,dt_1\right], \tag{29}$$

$$\langle \dot{X}(t+\tau)\dot{Y}(t)\rangle_{as} = -2D\rho \mathrm{Re}\left\{e^{i\Omega t}\left[\int_0^t e^{-i\Omega t_1}\ddot{H}(t_1+\tau)\dot{\psi}(t_1)\,dt_1 - \int_0^{\tau} e^{i\Omega t_1}\ddot{H}(\tau-t_1)\dot{\psi}(t_1)\,dt_1\right]\right\}, \tag{30}$$

$$\langle \dot{X}(t+\tau)\dot{X}(t)\rangle_{as} = -2D\ddot{\psi}(\tau) + \frac{\rho^2\langle y_0^2\rangle}{2}|\hat{\ddot{H}}(-i\Omega)|^2\{\cos(\Omega\tau) + \cos[\Omega(2t+\tau)+2\varphi]\} + D\rho^2\{\mathrm{Re}[B_0(\tau,\Omega)] + |B_1(\tau,\Omega)|\cos[2\Omega t+\varphi_1(\tau)]\}, \tag{31}$$

where

$$B_j(\tau,\Omega) = \int_0^{\infty} e^{-i2j\Omega t}[\ddot{H}(t)N(t+\tau) + \ddot{H}(t+\tau)N(t)]\,dt, \quad j = 0,1, \tag{32}$$

$$N(t) = \int_0^t e^{i\Omega t_1}\ddot{H}(t-t_1)\psi(t_1)\,dt_1,$$

and

$$\tan[\varphi_1(\tau)] = \frac{\mathrm{Im}[B_1(\tau,\Omega)]}{\mathrm{Re}[B_1(\tau,\Omega)]}. \tag{33}$$

The autocorrelation of velocity fluctuations $\langle \dot{X}(t+\tau)\dot{X}(t)\rangle_{as}$ in the flow direction depends on the shear rate ρ, the noise intensity D, the shear frequency Ω, and the initial positional variance $\langle y_0^2\rangle$ in y direction. It is important to note that in the long-time limit memory about the initial positional distribution in y direction will not vanish.

Now we consider the asymptotic evolution of the VCFs at large values of the lag time $\tau \gg \gamma^{-\frac{1}{2-\alpha}}$. Taking into account Eqs. (29)–(32), one can use (A2) and (A5) to obtain at $\tau \to \infty$

$$\langle \dot{Y}(t)\dot{Y}(t+\tau)\rangle_{as} \simeq -2D\ddot{\psi}(\tau), \tag{34}$$

$$\langle \dot{Y}(t+\tau)\dot{X}(t)\rangle_{as} \simeq -2D\rho\dot{\psi}(\tau)|\hat{\ddot{H}}(-i\Omega)|\cos(\Omega t+\varphi), \tag{35}$$

$$\langle \dot{Y}(t)\dot{X}(t+\tau)\rangle_{as} \simeq 2D\rho\dot{\psi}(\tau)|\hat{\ddot{H}}(-i\Omega)|\cos[\Omega(t+\tau)+\varphi], \tag{36}$$

$$\langle \dot{X}(t)\dot{X}(t+\tau)\rangle_{as} \simeq \frac{\rho^2}{2}|\hat{\ddot{H}}(-i\Omega)|^2\left[\langle y_0^2\rangle + 2D\psi(\tau)\right] \times\{\cos(\Omega\tau) + \cos[\Omega(2t+\tau)+2\varphi]\} \tag{37}$$

[see also Eq. (27)]. From Eqs. (34)–(37) it is seen that differently from other correlation functions, which by increasing τ tend to zero as a power law, the autocorrelation of velocity fluctuations in the flow direction tends to periodic functions on both times t and τ with a finite amplitude $\rho^2\langle y_0^2\rangle|\hat{\ddot{H}}(-i\Omega)|^2/2$. Thus, the asymptotic behavior of $\langle \dot{X}(t)\dot{X}(t+\tau)\rangle_{as}$ is the same as in the case without external noise ($D = 0$) [see Eq. (31)].

Figures 1 and 2 depict the typical dependencies of VCFs $C_{ij}^V(\tau)$ on small and moderate values of the lag time τ. From Fig. 1 it is seen that the exact solution for $C_{11}^V(\tau)$ exhibits exponentially damped oscillations around a curve which for large τ decays absolutely monotonically like a power law with the exponent $2\alpha - \delta$. Consequently, the autocorrelation function $C_{11}^V(\tau)$ is characterized by a finite number of zeros. A comparison with Eqs. (A3)–(A6) shows that there is an important characteristic time τ_1,

$$\tau_1 = \frac{1}{\beta} = -\gamma^{-\frac{1}{2-\alpha}}\frac{1}{\cos\left(\frac{\pi}{2-\alpha}\right)}. \tag{38}$$

If τ is small or comparable with τ_1, then the oscillatory behavior of $C_{11}^V(\tau)$ with a frequency $\omega = \gamma^{\frac{1}{2-\alpha}}\sin(\frac{\pi}{2-\alpha})$ is important, but in the time scale $\tau \gg \tau_1$ a power-law-like monotonic decay of $C_{11}^V(\tau)$ dominates.

For the cross-correlation functions $C_{12}^V(\tau)$ and $C_{21}^V(\tau)$ the dependence on small and moderate values of τ is more complicated: it realizes as a nonlinear interplay of three oscillatory motions with frequencies Ω and ω in times t and τ. More precisely, $C_{12}^V(\tau)$ includes a nonlinear superposition of the oscillations of the shear flow in time t (frequency Ω) and the relaxation oscillations in time τ with a frequency

$$\omega = \gamma^{\frac{1}{2-\alpha}}\sin\left(\frac{\pi}{2-\alpha}\right), \tag{39}$$

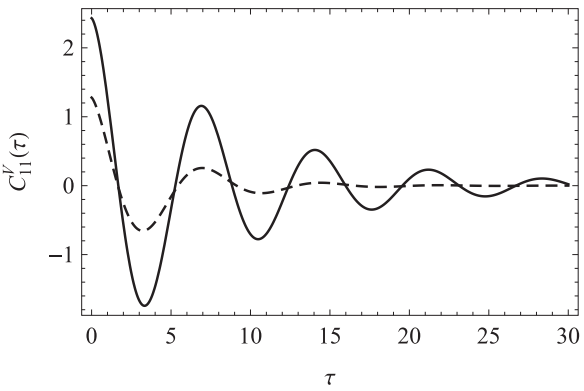

FIG. 1. Dependence of the autocorrelation function $C_{11}^V(\tau) = \langle \dot{Y}(t+\tau)\dot{Y}(t)\rangle_{as}$ on the time lag τ computed from Eqs. (23) and (A5) at different values of the memory exponent α. Parameter values: $D = 0.5$, $\gamma = 0.8$, and $\delta = 0.8$. Solid line, $\alpha = 0.15$; dashed line, $\alpha = 0.3$.

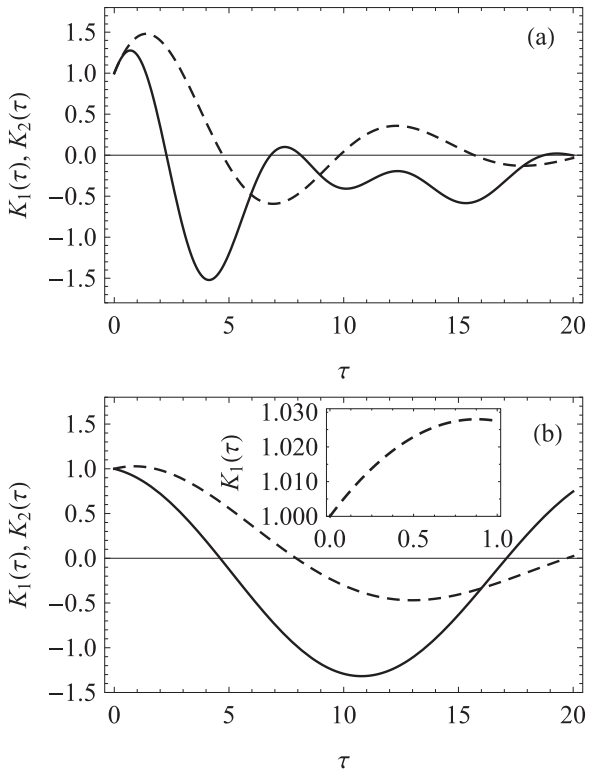

FIG. 2. Normalized cross-correlation functions $K_1(\tau) = C_{12}^V(\tau)/C_{21}^V(0)$ and $K_2(\tau) = C_{21}^V(\tau)/C_{21}^V(0)$ vs the time lag τ computed from Eqs. (29), (30), (A2), (A5), and (B1). Parameter values: $t = 2\pi n/\Omega$, n an integer, $\rho = 1$, $D = 0.5$, $\alpha = 0.25$, and $\delta = 0.9$. The solid line and the dashed line correspond to the dependence of $K_2(\tau)$ and $K_1(\tau)$ on the time lag τ, respectively. (a) $\gamma = 0.4$ and $\Omega = 0.5$; the cross-correlation $C_{21}^V(0) \approx -1.023$. (b) $\gamma = 0.1$ and $\Omega = 0.01$; $C_{21}^V(0) \approx -28.27$. The inset emphasizes the slight increase of $K_1(\tau)$ at small values of τ. More details are given in the text.

but $C_{21}^V(\tau)$ depends, in addition, also on the shear flow oscillations in time τ [see also Eqs. (35) and (36)]. Here we emphasize that in a quiescent fluid cross-correlations between particle velocities in orthogonal directions vanish, i.e., $C_{21}^V(\tau) = C_{12}^V(\tau) = 0$, but shear flow causes finite cross-correlations in the shear plane [25,29]. Any translation of a particle in the y direction is coupled via the flow profile (1) to a change of the particle's velocity in the x direction, which leads to a change of the particle's velocity fluctuations along the x direction. Consequently the particle's velocity fluctuations in the x and y directions become correlated due to the shear flow. Figure 2 demonstrates at $t = 2\pi n/\Omega$, while n is an integer, a shear-induced asymmetry of the cross-correlation functions $C_{21}^V(\tau) \neq C_{12}^V(\tau)$ with respect to the time lag τ [see also Eqs. (29) and (32)]. The time asymmetry of $C_{12}^V(\tau)$ and $C_{21}^V(\tau)$ manifests itself more clearly in the case of a nonoscillatory shear flow, $\Omega = 0$. For large values of the lag time τ, using that at $\Omega = 0$ the phase shift $\varphi = \pi$, it is easy to see from Eqs. (27), (35), and (36) that $C_{12}^V(\tau)$ and $C_{21}^V(\tau)$ decay with long negative and positive tails, respectively:

$$C_{12}^V(\tau) \simeq 2D\rho\dot{\psi}(\tau), \quad C_{21}^V(\tau) \simeq -2D\rho\dot{\psi}(\tau), \quad \tau \to \infty. \tag{40}$$

Alternatively, at small times, $\tau \ll \{2\pi/\omega, \tau_1\}$, it follows from Eqs. (29) and (30) that

$$C_{12}^V(\tau) \approx C_{12}^V(0) - R\tau \tag{41}$$

and

$$C_{21}^V(\tau) \approx C_{12}^V(0) + R\tau, \quad \tau \to 0, \tag{42}$$

with

$$R = 2D\rho \int_0^\infty \ddot{H}(t)\ddot{\psi}(t)\,dt > 0. \tag{43}$$

Thus, during an initial period of lag time shorter than the relaxation time τ_1, the cross-correlation function $C_{21}^V(\tau)$ grows, while $C_{12}^V(\tau)$ decays [see also Fig. 2(b)]. It should be noted that in a recent experiment [29] a shear-induced asymmetry with respect to the time lag τ of the cross-correlation functions of particle positional fluctuations perpendicular to and along streamlines in the case of internal noise with Stokes friction was established.

To emphasize the dynamical differences between the systems with external noise and with internal noise ($\delta = \alpha$) we note that although in both cases the velocity process in the y direction $\dot{Y}(t)$ is a stationary process with the autocorrelation function determined by Eq. (23), a substantial difference occurs for the process $\dot{X}(t)$. Namely, in the case of external noise all second-order moments of the output [including $\langle[\dot{X}(t)]^2\rangle$] are, by condition (26), bounded in the long-time limit, but in the case of internal noise the velocity process $\dot{X}(t)$ is subdiffusive, i.e.,

$$\langle[\dot{X}(t)]^2\rangle \simeq \frac{kT\rho^2 t^\alpha}{\gamma\Gamma(1+\alpha)}|\hat{\ddot{H}}(-i\Omega)|^2\{1+\cos[2(\Omega t+\varphi)]\}, \quad t \to \infty, \tag{44}$$

where T is the absolute temperature of the heat bath and k is the Boltzmann constant.

IV. RESONANCES

In Eq. (2) the shear flow ($\Omega \neq 0$) can be considered as an external periodic driving force. As such, it allows excitation of internal modes of the unperturbed system [28].

A. Long lag time regime

In the long lag time regime, $\tau \to \infty$, the nonmonotonic dependence of the amplitudes of the oscillating velocity correlation functions on the frequency Ω is determined by the factor $|\hat{\ddot{H}}(-i\Omega)|$ in Eqs. (35)–(37). The corresponding position of the resonant maximum is given by (see also Fig. 3)

$$\Omega_{ex} = \left[\gamma\cos\left(\frac{\pi\alpha}{2}\right)\right]^{\frac{1}{2-\alpha}}. \tag{45}$$

The maximal value of $|\hat{\ddot{H}}(-i\Omega)|$ reads as

$$|\hat{\ddot{H}}(-i\Omega_{ex})| = \frac{1}{\sin\left(\frac{\pi\alpha}{2}\right)}. \tag{46}$$

So, from Eqs. (35)–(37) and (A5), a strong resonance of the velocity correlation functions is expected. This effect gets more and more pronounced as the memory exponent α

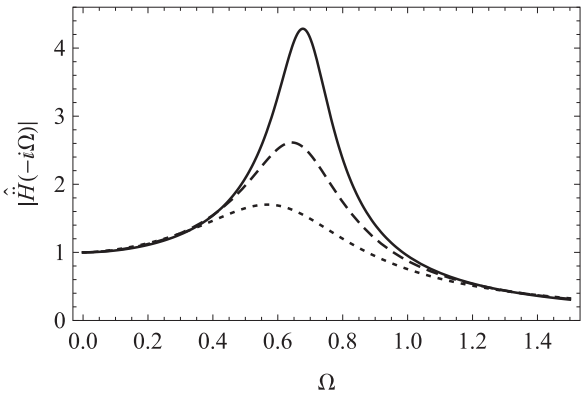

FIG. 3. Dependence of the amplitude factor $|\hat{\tilde{H}}(-i\Omega)|$ of the VCFs on the shear flow frequency Ω at the long lag time limit [Eqs. (35)–(37) and (A1)]. Solid line, $\alpha = 0.15$; dashed line, $\alpha = 0.25$; dotted line, $\alpha = 0.4$. The damping coefficient $\gamma = 0.5$.

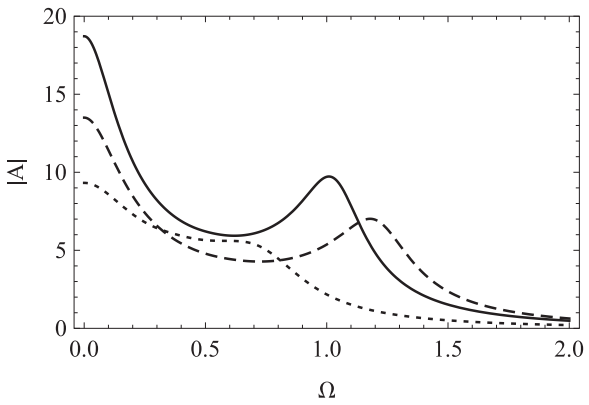

FIG. 4. Amplitude $|A|$ of the velocity cross-moment $\langle \dot{Y}(t)\dot{X}(t)\rangle_{as}$ as a function of the shear flow frequency Ω computed from Eq. (B1) at $\delta = 0.9$. Solid line, $\alpha = 0.15$ and $\gamma = 0.3$; dashed line, $\alpha = 0.15$ and $\gamma = 0.5$; dotted line, $\alpha = 0.3$ and $\gamma = 0.2$.

decreases. This result of resonance for a free particle is highly unexpected, but agrees well with the description of the friction force for small α as an elastic force due to the cage effect [23]. The increase of resonant peaks by decreasing α is caused from a decrease of the effective damping coefficient β [see also Eqs. (38) and (A5)]. The occurrence of a resonance is in agreement with Eqs. (5) and (6) for particle displacements and emphasizes that such a resonance is not due to any specific properties of the measured quantity but rather to a complex interaction of the particle with the medium as described by the memory term.

B. Second moments

We now explicitly consider the velocity moments $C^V_{ij}(0)$, where resonance effects are manifested as amplitude peaks at particular shear frequencies Ω. Since the velocity component $\dot{Y}(t)$ is not affected by shear flow, its second moment $\langle \dot{Y}^2\rangle_{as}$ is a constant; see Eq. (23). Starting from Eq. (29) we obtain the following formula for the cross-moment $\langle \dot{Y}(t)\dot{X}(t)\rangle_{as}$:

$$\langle \dot{Y}(t)\dot{X}(t)\rangle_{as} = -2D\rho|A(\Omega)|\cos(\Omega t + \varphi_2), \tag{47}$$

where

$$A(\Omega) := \int_0^\infty e^{-i\Omega t}\,\ddot{H}(t)\dot{\psi}(t)\,dt, \tag{48}$$

and

$$\tan\varphi_2 = \frac{\mathrm{Im}[A(\Omega)]}{\mathrm{Re}[A(\Omega)]}. \tag{49}$$

The exact formulas convenient for a numerical treatment of the quantities $A(\Omega)$ and $B_j(\Omega)$ are given by Eqs. (B1) and (B2) (see Appendix B). The dependence of the amplitude $|A(\Omega)|$ of the cross-moment $\langle \dot{X}(t)\dot{Y}(t)\rangle_{as}$ on the frequency Ω is shown in Fig. 4 for different values of the memory exponent α and the damping coefficient γ. These graphs show a typical resonance, with nonmonotonic behavior for the frequencies Ω close to several resonance frequencies, which is a bona fide resonance phenomenon. For sufficiently small values of the memory exponent α the amplitude $|A(\Omega)|$ exhibits a clear resonance near $\Omega = 2\omega$ [see Eq. (39)], which becomes less pronounced as the memory exponent increases. It is easily verified [by plotting Eq. (B1)] that there exists a critical memory exponent α_c which marks a transition between the resonant regime ($\alpha < \alpha_c$) and a dynamical regime where resonance is impossible. Actually, using that by time scaling $\tilde{t} = \gamma^{\frac{1}{2-\alpha}}t$ the amplitude $A(\Omega,\gamma)$ and the frequency Ω obey the scaling laws

$$A(\Omega,\gamma) = \gamma^{\frac{\delta-3}{2-\alpha}}A(\tilde{\Omega},1), \quad \tilde{\Omega} = \gamma^{-\frac{1}{2-\alpha}}\Omega, \tag{50}$$

we obtain that the critical memory exponent depends only on the noise exponent δ, i.e., $\alpha_c = \alpha_c(\delta)$. It is important to note that the value of α_c is quite robust: it decreases very slowly from $\alpha_c(0.99) \approx 0.31$ to $\alpha_c(0.58) \approx 0.29$ as δ decreases. Moreover, as the bounded regime is possible only if $\alpha < \delta/2$ [see Eq. (26)], it follows that by conditions (26) there is a lower limit $\delta_c \approx 0.58$ for the value of the exponent δ below which the resonance appears at all values of α and γ. The existence of $\alpha_c(\delta)$ can be qualitatively understood considering that the memory-generated effective damping β increases by increasing α [see Eq. (38)]. In the high-frequency limit the amplitude goes to zero, i.e., in this case the particles are too inert to adjust to the motion of the flow. In the nonoscillatory limit, $\Omega \to 0$, $|A(\Omega)|$ approaches a finite value which is the maximal value of $|A(\Omega)|$ by fixed values of the other parameters. The last mentioned circumstance is in contrast with the results of Ref. [28], where it is shown that in the case of Stokes friction ($\alpha = 1$) for an oscillatory shear flow model with an internal noise and with a harmonic trapping potential, the particles' velocity cross-correlation tends to zero as $\Omega \to 0$.

We now consider the second moment $\langle \dot{X}^2(t)\rangle_{as}$, where the multiresonance effect occurs [see Eq. (31)]. First, we examine the resonance phenomenon for the term $\mathrm{Re}[B_0(\Omega)]$ in Eq. (31). In Fig. 5 several graphs depict the behavior of $\mathrm{Re}[B_0(\Omega)]$ versus Ω for different representative values of the memory exponent α and the noise exponent δ. One should discern two regions of α values separated with a critical memory exponent $\alpha_{c1}(\delta)$ (see Fig. 5). If $\alpha_{c1}(\delta) < \alpha < \delta/2$, the quantity $\mathrm{Re}(B_0)$ is characterized with one resonant peak at the frequency of the relaxation oscillations, $\Omega \approx \omega$. This peak grows rapidly as the memory exponent α tends to the instability limit ($\alpha = \delta/2$). If $\alpha < \alpha_{c1}(\delta)$, $\mathrm{Re}(B_0)$ exhibits two resonance

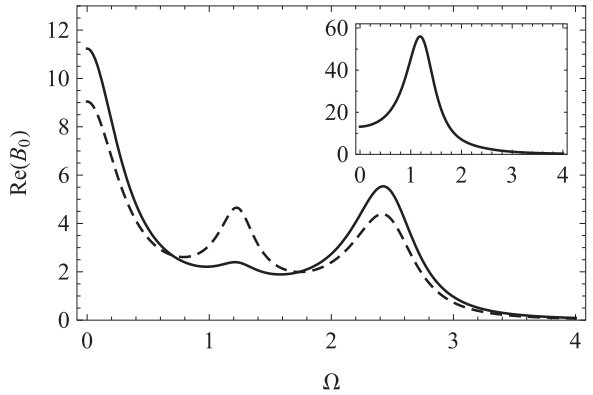

FIG. 5. Multiresonance of the second moment $\langle \dot{X}^2(t)\rangle_{as}$ characteristic Re$[B_0(\Omega)]$ [see Eq. (31)], computed from Eq. (B2) at $\gamma = 1.5$. Solid line: $\delta = 0.9$ and $\alpha = 0.15$; dashed line: $\delta = 0.61$ and $\alpha = 0.15$. The inset depicts the resonant behavior of Re(B_0) versus the frequency Ω of the shear flow at parameter values: $\gamma = 1.5$, $\delta = 0.61$, and $\alpha = 0.3$ (i.e., $\alpha > \alpha_{c1} \approx 0.234$). More details are given in the text.

peaks, at $\Omega \approx \omega$ and $\Omega \approx 2\omega$; i.e., a multiresonance occurs. The peak near the double relaxation frequency, $\Omega = 2\omega$, becomes the dominant resonance at small values of α. As the memory exponent α tends to zero the resonant maximum at $\Omega \approx 2\omega$ tends to infinity. The last mentioned circumstance is in agreement with the fact that in the limit $\alpha \to 0$ the effective damping coefficient β will vanish. Evidently, if $\delta < 2\alpha_{c1}(\delta)$, the multiresonance regime occurs at all values of α and γ $(0 < \alpha < \delta/2)$.

The amplitude $|B_1|$ for the time-dependent contribution to $\langle \dot{X}^2(t)\rangle_{as}$ [see Eq. (31)] also has a two-peak structure by small values of the memory exponent α (see Fig. 6). The resonances appear at the frequencies $\Omega \approx 2\omega$ and $\Omega \approx \omega$. Although the peak at $\Omega \approx \omega$ tends to dominate, at sufficiently small values of the memory exponent α the peak at $\Omega = 2\omega$ can become the dominant resonance.

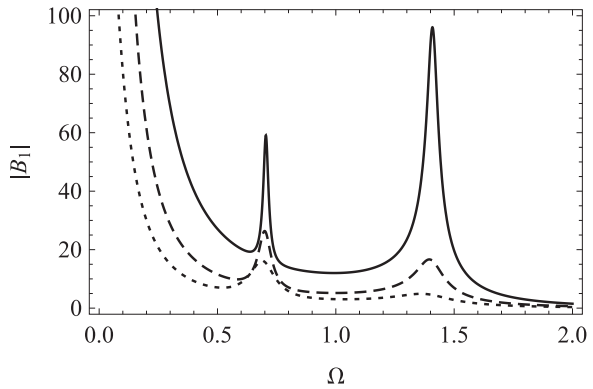

FIG. 6. Multiresonance-like dependence of the amplitude $|B_1|$ of $\langle \dot{X}^2\rangle_{as}$ on the shear flow frequency Ω at small values of the memory exponent α [cf. Eq. (31)]. The amplitude $|B_1|$ is computed from Eq. (B2) with $\gamma = 0.5$ and $\delta = 0.9$. Solid line: $\alpha = 0.02$, $|B_1(0)| \approx 23840$; dashed line: $\alpha = 0.05$, $|B_1(0)| \approx 1586$, dotted line: $\alpha = 0.1$, $|B_1(0)| \approx 215$.

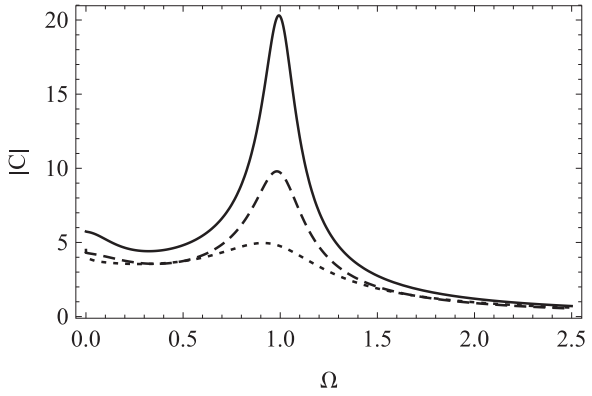

FIG. 7. Resonance for the particle angular momentum $\langle L_z\rangle$ versus the shear flow frequency Ω at $\langle y_0^2\rangle = 0$ for different values of the memory exponent α [see Eq. (51)]. The amplitude $|C|$ of $\langle L_z\rangle$ is computed from Eq. (B5) with $\gamma = 1$ and $\delta = 0.8$. Solid line, $\alpha = 0.1$; dashed line, $\alpha = 0.15$; dotted line, $\alpha = 0.3$. At high values of the shear flow frequency, $\Omega \to \infty$, the amplitude $|C|$ tends to zero.

It should be noted that both the term Re(B_0) and the amplitude $|B_1|$ attain finite values (sometimes very great values) at $\Omega = 0$ and vanish in the limit $\Omega \to \infty$.

Our next task is to examine the mean angular momentum $\langle L_z(t)\rangle = \langle X(t)\dot{Y}(t) - Y(t)\dot{X}(t)\rangle_{as}$ of particles in the shear flow. For model (2) it is given by

$$\langle L_z(t)\rangle = \rho\langle y_0^2\rangle|\hat{\tilde{H}}(-i\Omega)|\cos(\Omega t + \varphi) - 2D\rho\gamma|C(\Omega)|\cos(\Omega t + \varphi_3), \tag{51}$$

where

$$C(\Omega) = -\frac{1}{\gamma}\int_0^\infty e^{-i\Omega t}\psi(t)\{2\ddot{H}(t) + i\Omega[1 - \dot{H}(t)]\}\,dt \tag{52}$$

and

$$\tan\varphi_3 = \frac{\mathrm{Im}[C(\Omega)]}{\mathrm{Re}[C(\Omega)]} \tag{53}$$

[see also Eq. (B5) in Appendix B]. In the case of $\langle y_0^2\rangle = 0$, the results for the particle angular momentum are illustrated in Fig. 7. Before commenting on the resonance of the angular momentum $\langle L_z\rangle$, we note that in the case of the model with Stokes friction and with the trapping potential considered in Ref. [28] the amplitude of $\langle L_z\rangle$ decreases monotonically as Ω increases, i.e., the resonance is absent. For our model (2) the resonance of $\langle L_z\rangle$ occurs at $\Omega \approx \omega$, i.e., when the shear flow frequency Ω and the relaxation frequency ω [see Eq. (39)] coincide. The effect exists by all values of other system parameters and is more pronounced at small values of the memory exponent.

It is important to note that in the absence of the driving noise $\boldsymbol{\xi}(t)$, $D = 0$, the angular momentum $\langle L_z\rangle$ is proportional to the variance $\langle y_0^2\rangle$ of the initial particle coordinate in the y direction [see Eq. (51)]. In this case, if $\langle y_0^2\rangle \neq 0$, $\langle L_z\rangle$ exhibits a resonance at $\Omega \approx \Omega_{ex}$ [see Eq. (45) and Fig. 3]. Thus, in the general case, $D \neq 0$ and $\langle y_0^2\rangle \neq 0$, the model (2) predicts a double resonance of $\langle L_z\rangle$, with the peaks at $\Omega = \Omega_{ex}$ and $\Omega \approx \omega$.

Finally, we consider, in brief, the case where $\boldsymbol{\xi}(t)$ in Eq. (2) is replaced with a superposition of the external noise and the internal noise. The main ingredient which determines the long-time behavior of VCFs and $\langle L_z\rangle$ is the second moment of the particle coordinate in the y direction $\langle Y^2(t)\rangle_{as}$. In the long-time limit, $t\to\infty$, we obtain

$$\langle Y^2(t)\rangle_{ex} = 2D\psi(0), \quad \langle Y^2(t)\rangle_{\rm in} \simeq \frac{2kT}{\gamma\Gamma(1+\alpha)}t^{\alpha}, \qquad (54)$$

where $\langle Y^2(t)\rangle_{ex}$ and $\langle Y^2(t)\rangle_{\rm in}$ correspond to the cases of external and internal noises, respectively. From Eq. (54) a new characteristic time τ_2 can be introduced,

$$\tau_2 = \left[\frac{D\psi(0)\gamma}{kT}\right]^{\frac{1}{\alpha}}. \qquad (55)$$

If the relative intensity of the external noise and the internal noise is great enough, then the inequality $\tau_1 \ll \tau_2$ is possible [see also Eq. (38)]. It can be shown that in the time scale

$$\tau_1 \ll t \ll \tau_2 \qquad (56)$$

all results obtained in this paper remain applicable. In this case the influence of the internal noise appears in the time scale $t \gtrsim \tau_2$.

V. CONCLUSIONS

On the basis of a generalized Langevin equation with a power-law memory kernel we have analyzed the behavior of the velocity correlation functions and the angular momentum of a "free" underdamped Brownian particle embedded in a viscoelastic oscillatory shear flow. Its interaction with fluctuations of environmental parameters is modeled by an external additive fractional Gaussian noise with an exponent δ.

As our main result we have established, in the long-time regime, a cage effect (see Ref. [23]) induced trapped (confined) regime of the velocity process of the Brownian particle, which is characterized with a bounded variability of the VCFs and the particle's mean angular momentum. Such a trapped regime is possible if the memory exponent $\alpha < 1/2$ and if the exponent δ characterizing the external noise fulfils the inequality $2\alpha < \delta < 1$. Note that in the case of an internal noise the corresponding velocity process in the shear flow directions is always subdiffusive, i.e., unbounded.

Particularly, we have found that in the case of confined dynamics of the particle's velocity process an interplay of the external noise, the shear flow, and memory effects can generate a rich variety of nonequilibrium cooperation phenomena. Those include, for example, (i) at large values of the lag time, a strong dependence of the asymptotic velocity autocorrelation function in the shear flow direction as well as the angular momentum on the initial positional distribution of particles; (ii) in the long-time limit, an oscillatory behavior of VCFs in time t, which demonstrates a clear resonance at a certain value of the shear flow frequency Ω; (iii) a qualitative difference between the dependencies of cross-correlation functions $\langle\dot X(t)\dot Y(t+\tau)\rangle_{as}$ and $\langle\dot X(t+\tau)\dot Y(t)\rangle_{as}$ on the lag time τ; (iv) double resonance of the second-order velocity moment in the shear flow direction $\langle\dot X^2(t)\rangle_{as}$ at $\Omega\approx\omega$ and $\Omega\approx 2\omega$ (the relaxation frequency ω depends only on the parameters of the memory kernel); (v) a strong resonance of the mean angular momentum $\langle L_z\rangle$ of Brownian particles at $\Omega\approx\omega$; and (vi) the resonance of $\langle L_z\rangle$ and $\langle\dot X^2(t)\rangle_{as}$ versus Ω (related to the initial positional distribution of particles), even if external noise is absent.

It should be noted that previously the resonant behavior of the VCFs vs Ω for a harmonically trapped Brownian particle embedded in the oscillatory shear flow with Stokes friction was considered in Ref. [28], but that model (with internal noise) is qualitatively different from the one considered in our paper. Thus, the results presented here and in Ref. [28] are also different, e.g., for the model in Ref. [28] the amplitude of $\langle L_z\rangle$ is a decreasing function of Ω; i.e., the resonance is absent. As in most resonant effects considered here the positions of the resonant peaks appear at $\Omega=\omega$ and/or $\Omega=2\omega$ wherein ω depends only on parameters of the memory kernel, it seems that these effects could be used in microrheology experiments to analyze viscoelastic properties of media.

Finally, we believe that our results suggest some possibilities for interpreting experimental data in applications where the issues of viscoelasticity and external noise can be crucial, e.g., for particles in dusty plasmas [9] and in the cytoplasm of cells [7,8,32].

ACKNOWLEDGMENTS

The work was supported by the Estonian Science Foundation under Grant No. 9005, by the Ministry of Education and Research of Estonia under Grant No. SF0130010s12, by the International Atomic Energy Agency under Grant No. 16931, and by the European Union through the European Regional Development Fund (Estonian Center of Excellence "Mesosystems–Theory and Applications," TK114).

APPENDIX A: FORMULAS FOR THE CORRELATION FUNCTION $\psi(\tau)$

To derive a convenient representation of $\psi(\tau)$ defined by Eq. (24), we start from a Laplace transform $\widehat{H}(s)$ of the relaxation function $H(t)$ [see also Eq. (12)]:

$$\widehat{H}(s) = \frac{s^{-\alpha}}{s^{2-\alpha}+\gamma}. \qquad (A1)$$

Using the residue theorem method described in Ref. [42], the inverse Laplace transform gives

$$H(t) = \frac{\gamma\sin(\pi\alpha)}{\pi}\int_0^{\infty}\frac{e^{-rt}dr}{r^{\alpha}B(r)} + \frac{2e^{-\beta t}}{(2-\alpha)\gamma^{\frac{1}{2-\alpha}}}\mathrm{Im}[e^{i(\omega t+\Theta)}], \qquad (A2)$$

where

$$\beta = -\gamma^{\frac{1}{2-\alpha}}\cos\left(\frac{\pi}{2-\alpha}\right), \quad \omega = \gamma^{\frac{1}{2-\alpha}}\sin\left(\frac{\pi}{2-\alpha}\right),$$
$$B(r) = r^{2(2-\alpha)} + 2\gamma r^{2-\alpha}\cos(\pi\alpha) + \gamma^2, \qquad (A3)$$
$$\Theta = -\frac{\pi\alpha}{2(2-\alpha)}.$$

The behavior of the asymptotic correlation function $\langle Y(t)Y(t+\tau)\rangle_{as}\sim\psi(\tau)$ is more subtle. It follows from Eqs. (3), (24), (25), and (A2) that we have, depending on the values of the exponents $0<\delta<1$ and $0<\alpha<1$, three

different cases. The possible limiting behaviors of the second moment $\langle Y^2(t)\rangle$ at $t \to \infty$ are (see also Ref. [20])

$$\langle Y^2(t)\rangle \sim \begin{cases} \text{const}, & \delta > 2\alpha \quad \text{(stationary)} \\ \ln t, & \delta = 2\alpha \quad \text{(logarithmic)} \\ t^{2\alpha-\delta}, & \delta < 2\alpha \quad \text{(anomalous diffusion)}. \end{cases} \tag{A4}$$

In the case where $\delta < 2\alpha$ we distinguish three different regimes for the process $Y(t)$: (i) subdiffusion, if $2\alpha > \delta > 2\alpha - 1$; (ii) normal diffusion, if $\delta = 2\alpha - 1$; and (iii) superdiffusion, if $\delta < 2\alpha - 1$.

In the stationary regime ($t \to \infty$), $1 > \delta > 2\alpha$, we obtain

$$\psi(\tau) = \frac{\gamma \sin(\pi\alpha)}{\pi} \int_0^\infty \frac{e^{-r\tau}\,\widehat{H}(r) f(r)\,dr}{r^\alpha B(r)} + \frac{2}{(2-\alpha)\gamma^{\frac{1}{2-\alpha}}} \times \mathrm{Im}[f(\beta - i\omega)\widehat{H}(\beta - i\omega)e^{i\Theta}e^{-(\beta - i\omega)\tau}], \tag{A5}$$

with

$$f(r) := \frac{2r^{\delta-1}\sin\left(\frac{\pi\delta}{2}\right)}{\gamma \sin(\pi\alpha)} \left\{ r^{2-\alpha}\cos\left(\frac{\pi\delta}{2}\right) + \gamma \cos\left[\frac{\pi(\delta - 2\alpha)}{2}\right]\right\}. \tag{A6}$$

We note that although the formula (A5) is valid only for $\delta > 2\alpha$, it follows from Eq. (24) that for $\ddot{\psi}(\tau)$ an analogous formula obtained from Eq. (A5) by differentiation is more general, i.e., it is true for all values of the exponents, $0 < \delta < 1$ and $0 < \alpha < 1$.

APPENDIX B: FORMULAS FOR SECOND MOMENTS

Here the exact expressions for the computation of the quantities $A(\Omega)$, $B_j(0,\Omega)$, and $C(\Omega)$, which determine the long-time behavior of the second moments, are presented. From Eqs. (32), (48), (A2), and (A5) it can be concluded that $A(\Omega)$ and $B_j(0,\Omega)$ are given by

$$A(\Omega) = \frac{\gamma^2 \sin(\pi\alpha)}{\pi} \int_0^\infty \frac{\widehat{H}(r)\widehat{\chi}(r + i\Omega) f(r) r^{1-\alpha}\,dr}{B(r)} + \frac{\gamma^{\frac{1-\alpha}{2-\alpha}}}{(2-\alpha)i}\{(\beta - i\omega) f(\beta - i\omega)\widehat{H}(\beta - i\omega)\widehat{\chi}[\beta - i(\omega - \Omega)]e^{i\Theta} - (\beta + i\omega) f(\beta + i\omega)\widehat{H}(\beta + i\omega)\widehat{\chi}[\beta + i(\omega + \Omega)]e^{-i\Theta}\} \tag{B1}$$

and

$$B_j(0,\Omega) = -\frac{2\gamma^2 \sin(\pi\alpha)}{\pi} \int_0^\infty \frac{r^{2-\alpha}\widehat{\chi}(r + i2j\Omega)}{B(r)} \widehat{\psi}[r + i\Omega(2j-1)]\,dr - \frac{2\gamma^{\frac{1-\alpha}{2-\alpha}}}{(2-\alpha)i}\{(\beta - i\omega)^2 e^{i\Theta}\widehat{\chi}[\beta - i(\omega - 2j\Omega)]\widehat{\psi}\{\beta - i[\omega - (2j-1)\Omega]\} - (\beta + i\omega)^2 e^{-i\Theta}\widehat{\chi}[\beta + i(\omega + 2j\Omega)]\widehat{\psi}\{\beta + i[\omega + (2j-1)\Omega]\}\}, \quad j = 0,1, \tag{B2}$$

where

$$\widehat{\psi}(s) = \frac{\gamma \sin(\pi\alpha)}{\pi} \int_0^\infty \frac{f(r)\widehat{H}(r)\,dr}{r^\alpha B(r)(s + r)} + \frac{1}{(2-\alpha)\gamma^{\frac{1}{2-\alpha}} i}\left[\frac{f(\beta - i\omega)e^{i\Theta}\widehat{H}(\beta - i\omega)}{\beta - i\omega + s} - \frac{f(\beta + i\omega)e^{-i\Theta}\widehat{H}(\beta + i\omega)}{\beta + i\omega + s}\right] \tag{B3}$$

and

$$\widehat{\chi}(s) = -\frac{1}{\gamma}\widehat{\dot{H}}(s) = \frac{1}{s^{2-\alpha} + \gamma}. \tag{B4}$$

Finally, using formulas (52), (A2), and (A5) we obtain for the complex amplitude $C(\Omega)$ of the angular momentum $\langle L_z\rangle$ [see Eq. (51)]

$$C(\Omega) = \frac{\gamma \sin(\pi\alpha)}{\pi} \int_0^\infty \frac{f(r)(2r + i\Omega)\widehat{H}(r)\widehat{\chi}(r + i\Omega)\,dr}{r^\alpha B(r)(r + i\Omega)} + \frac{1}{(2-\alpha)\gamma^{\frac{1}{2-\alpha}} i}\left\{\frac{f(\beta - i\omega)\widehat{H}(\beta - i\omega)e^{i\Theta}}{\beta - i(\omega - \Omega)}[2\beta - i(2\omega - \Omega)]\widehat{\chi}[\beta - i(\omega - \Omega)] - \frac{f(\beta + i\omega)\widehat{H}(\beta + i\omega)e^{-i\Theta}[2\beta + i(2\omega + \Omega)]}{\beta + i(\omega + \Omega)}\widehat{\chi}[\beta + i(\omega + \Omega)]\right\}. \tag{B5}$$

We have used Eqs. (B1), (B2), and (B5) to find the asymptotic behavior of the correlation functions [Eqs. (35)–(37)] as well as by analysis of the resonant behavior of second moments.

[1] F. Höfling and T. Franosch, Rep. Prog. Phys. **76**, 046602 (2013).
[2] W. Götze and L. Sjögren, Rep. Prog. Phys. **55**, 241 (1992).
[3] T. Carlsson, L. Sjögren, E. Mamontov, and K. Psiuk-Maksymowicz, Phys. Rev. E **75**, 031109 (2007).
[4] S. C. Weber, A. J. Spakowitz, and J. A. Theriot, Phys. Rev. Lett. **104**, 238102 (2010).
[5] Q. Gu, E. A. Schiff, S. Grebner, F. Wang, and R. Schwarz, Phys. Rev. Lett. **76**, 3196 (1996).
[6] I. Goychuk, Phys. Rev. E **80**, 046125 (2009).
[7] I. M. Tolić-Nørrelykke, E.-L. Munteanu, G. Thon, L. Oddershede, and K. Berg-Sørensen, Phys. Rev. Lett. **93**, 078102 (2004).
[8] R. Granek and J. Klafter, Phys. Rev. Lett. **95**, 098106 (2005).
[9] S. V. Muniandy, W. X. Chew, and C. S. Wong, Phys. Plasmas **18**, 013701 (2011).
[10] M. O. Magnasco, Phys. Rev. Lett. **71**, 1477 (1993).
[11] P. Reimann, Phys. Rep. **361**, 57 (2002).
[12] R. Mankin, R. Tammelo, and D. Martila, Phys. Rev. E **64**, 051114 (2001).
[13] L. Gammaitoni, P. Hänggi, P. Jung, and F. Marchesoni, Rev. Mod. Phys. **70**, 223 (1998).
[14] R. Benzi, A. Sutera, and A. Vulpiani, J. Phys. A **14**, L453 (1981).
[15] K. Laas, R. Mankin, and A. Rekker, Phys. Rev. E **79**, 051128 (2009).
[16] S. L. Ginzburg and M. A. Pustovoit, Phys. Rev. Lett. **80**, 4840 (1998).
[17] I. Bena, C. Van den Broeck, R. Kawai, and K. Lindenberg, Phys. Rev. E **66**, 045603(R) (2002).
[18] R. Mankin, A. Haljas, R. Tammelo, and D. Martila, Phys. Rev. E **68**, 011105 (2003).
[19] E. Lutz, Phys. Rev. E **64**, 051106 (2001).
[20] J. M. Porrá, K.-G. Wang, and J. Masoliver, Phys. Rev. E **53**, 5872 (1996).
[21] S. C. Kou and X. S. Xie, Phys. Rev. Lett. **93**, 180603 (2004).
[22] W. Min, G. Luo, B. J. Cherayil, S. C. Kou, and X. S. Xie, Phys. Rev. Lett. **94**, 198302 (2005).
[23] S. Burov and E. Barkai, Phys. Rev. E **78**, 031112 (2008).
[24] R. Rzehak and W. Zimmermann, Physica A **324**, 495 (2003).
[25] L. Holzer, J. Bammert, R. Rzehak, and W. Zimmermann, Phys. Rev. E **81**, 041124 (2010).
[26] J. Bammert and W. Zimmermann, Phys. Rev. E **82**, 052102 (2010).
[27] B. Lander, U. Seifert, and T. Speck, Phys. Rev. E **85**, 021103 (2012).
[28] H. Kählert and H. Löwen, Phys. Rev. E **86**, 041119 (2012).
[29] A. Ziehl, J. Bammert, L. Holzer, C. Wagner, and W. Zimmermann, Phys. Rev. Lett. **103**, 230602 (2009).
[30] I. Goychuk, Phys. Rev. E **76**, 040102 (2007).
[31] R. Mankin, K. Laas, and N. Lumi, Phys. Rev. E **88**, 042142 (2013).
[32] L. Bruno, V. Levi, M. Brunstein, and M. A. Despósito, Phys. Rev. E **80**, 011912 (2009).
[33] R. Mankin and A. Rekker, Phys. Rev. E **81**, 041122 (2010).
[34] R. Mankin, K. Laas, and A. Sauga, Phys. Rev. E **83**, 061131 (2011).
[35] P. Bursac, G. Lenormand, B. Fabry, M. Oliver, D. A. Weitz, V. Viasnoff, J. P. Butler, and J. J. Fredberg, Nature Mater. **4**, 557 (2005).
[36] A. W. C. Lau, B. D. Hoffmann, A. Davies, J. C. Crocker, and T. C. Lubensky, Phys. Rev. Lett. **91**, 198101 (2003).
[37] C. Wilhelm, Phys. Rev. Lett. **101**, 028101 (2008).
[38] M. A. Despósito and A. D. Viñales, Phys Rev. E **80**, 021111 (2009).
[39] T. A. Waigh, Rep. Prog. Phys. **68**, 685 (2005).
[40] R. Kubo, Rep. Prog. Phys. **29**, 255 (1966).
[41] I. Podlubny, *Fractional Differential Equations* (Academic Press, San Diego, 1999).
[42] S. Kempfle, J. Schäfer, and H. Beyer, Nonlinear Dyn. **29**, 99 (2002).